Implication of Baseband Impedance and Bias for FET Amplifier Linearization

James Brinkhoff and Anthony E. Parker

Department of Electronics, Macquarie University, Sydney AUSTRALIA 2109, Email:jamesb@ics.mq.edu.au

Abstract— **Baseband impedance can have a positive or negative effect on the intermodulation of microwave circuits. Concise formulae are shown to be useful to a designer to select intelligently a FET and its bias on the basis of the impact of baseband impedance on intermodulation. Memoryless predistortion techniques are shown to be effective over wide bandwidths at a suitable bias.**

I. Introduction

Wireless applications are requiring increasingly wideband amplifiers that are more linear. There are a number of methods used to linearize an amplifier, which mainly fall into the categories of feedforward, feedback, and predistortion. The predistortion technique is often used in mobile devices where cost and power usage are crucial. However, a fundamental problem is that predistortion is often very sensitive to memory effects in the amplifier. The distortion cancellation may be good for signals with small bandwidths, but poor for wideband signals because the intermodulation levels change with tone spacing [1].

Adaptive digital predistortion that seeks to compensate for the amplifier memory as well as intermodulation is one proposed solution to the problem of wideband linearization. This approach relies on complex formulation and signal processing [2]. Another possible approach is to devise circuit design techniques that minimize the dependence of intermodulation on baseband impedance. An example of this uses an injected baseband signal that compensates for the memory [3]. This technique can be effective, but it relies on additional, carefully tuned, circuit components. An alternative, simpler approach would be to operate the device in such a way that memory effects are minimized.

This work examines the bias dependence of the memory effects that are due to baseband impedance. It is shown that simply by careful selection of the operating point of a transistor, the memory effect due to baseband impedance can be minimized or maximized. The basis of this study is a Volterra-series analysis [4], which is summarized in Section II. The analysis is further developed here to produce two figures-of-merit for assessing the intermodulation behavior. This provides an understanding of, and ability to predict, bias and bandwidth dependence of intermodulation performance. In Section III, a pHEMT is characterized, and predictions and measurements of the effect of baseband impedance on intermodulation over a range of biases are compared. Finally, Section IV shows the linearization bandwidth achieved when data predistortion is applied to this transistor at different biases.

II. Intermodulation Model

An analysis has been previously developed to predict the effects of baseband impedance on intermodulation [4]. This analysis is valid for a FET in the common-source configuration with a two-tone input signal, where the impedance presented to the drain of the FET is $Z_d(\omega)$. Device capacitance effects have been neglected, however it will be shown in Section III that this does not compromise the usefulness of the analysis to predict the relative importance of baseband impedance effects. The results from the analysis are summarised in this section for completeness.

In [4] the drain current is described as a two-dimensional Taylor-series:

$$i_d = G_m v_g + G_d v_d + G_{m2} v_g^2 + G_{md} v_g v_d + G_{d2} v_d^2 + G_{m3} v_g^3 + G_{m2d} v_g^2 v_d + G_{md2} v_g v_d^2 + G_{d3} v_d^3 \quad (1)$$

Suppose that v_g is a two-tone signal, the magnitude of each tone being V_s, so that $v_g = 2V_s \cos(\omega_c)\cos(\Delta\omega/2)$. The carrier frequency ω_c is assumed to be much greater than the tone spacing $\Delta\omega$. The magnitude of the first-order output voltage at the fundamental frequencies is

$$V_{d1} = -V_s G_m Z_o(\omega_c) \quad (2)$$

$$Z_o(\omega) = \frac{Z_d(\omega)}{1 + G_d Z_d(\omega)} \quad (3)$$

is the drain conductance in parallel with the drain termination, and G_m and G_d are the first-order transconductance and drain conductance respectively.

The magnitude of the third-order output voltage at the intermodulation frequencies is

$$V_{d3} = V_s^3 Z_o(\omega_c)\Big(c_0 Z_o(\Delta\omega) + c_1 + c_2 Z_o(2\omega_c)\Big) \quad (4)$$

0-7803-7695-1/03/$17.00 © 2003 IEEE

where c_0, c_1 and c_2 are defined in [4]. They are dependent on the impedance at the fundamental frequency only, and change with bias because they involve the nine coefficients of the nonlinear drain current, (1).

It is the term $c_0 Z_o(\Delta\omega)$ in (4) that is dependent on the baseband drain impedance. Hence, if c_0 is very small at a certain bias, the intermodulation will be relatively constant even if the baseband impedance changes significantly over the range of tone spacings. The terms $c_1 + c_2 Z_o(2\omega_c)$ are dependent only on the impedances at the fundamental and second-harmonic frequencies.

Two figures-of-merit are proposed to enable the selection of a device and its bias based on its distortion performance. These figures-of-merit are an assessment of the absolute intermodulation level, and the effect of baseband impedance on intermodulation. They model the low-frequency behavior of a device very accurately, and as will be shown later, predict the overall trends of the intermodulation at high frequencies as well. They are very useful when computed over a range of biases.

The first figure-of-merit, IM3, is the intermodulation level relative to the fundamental level (dBc) with zero baseband drain termination ($Z_d(\Delta\omega) = 0$, as is often the case with LC bias networks at small tone spacings). With reference to (2) and (4), this quantity is:

$$\mathrm{IM3} = 20 \log \left| \frac{V_s^2}{G_m} (c_1 + c_2 Z_o(2\omega_c)) \right| \ [\mathrm{dBc}] \qquad (5)$$

The second figure-of-merit, ΔIM3, gives an indication of how much the intermodulation will change when the baseband impedance changes from 0 to some other value, Z_b. The equation for this is:

$$\Delta\mathrm{IM3} = 20 \log \left| \frac{c_0 \frac{Z_b}{1+G_d Z_b} + c_1 + c_2 Z_o(2\omega_c)}{c_1 + c_2 Z_o(2\omega_c)} \right| \ [\mathrm{dB}] \qquad (6)$$

Z_b is the nominal load, which for this work is 50 Ω. Thus, ΔIM3 indicates the change in the intermodulation levels as the baseband impedance changes from 0 Ω at small tone spacings, to the load impedance at large tone spacings (as is the case with the LC bias networks used).

III. pHEMT Characterization and Measurement

A packaged pHEMT device was characterized and the predicted and measured behavior compared. The nine coefficients of the Taylor-series expansion of drain-current were extracted using a two-tone distortion measurement method, similar to the one proposed in [5],

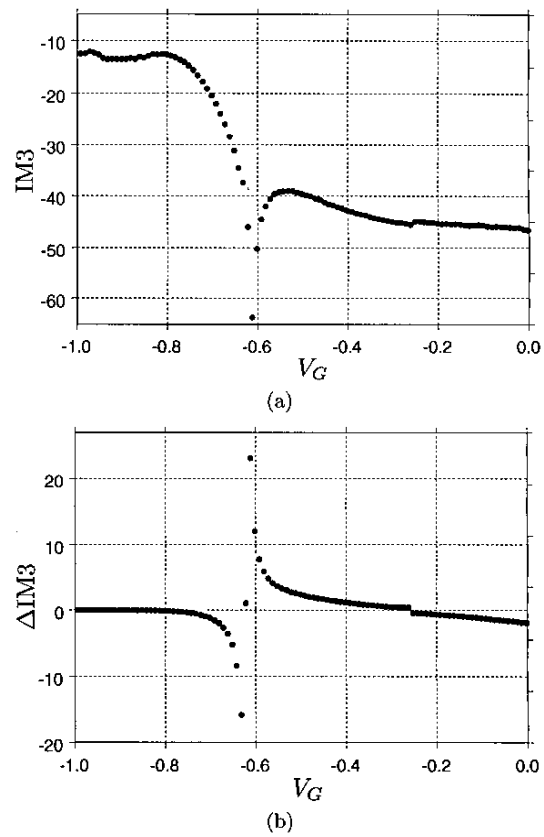

Fig. 1. The two figures-of-merit verses gate bias for a pHEMT with $V_D = 2$ V.
(a) Predicted intermodulation (dBc) with $Z_d(\Delta\omega) = 0$.
(b) Change in intermodulation (dB) when the baseband impedance changes from 0 to 50 Ω.

over 101 gate biases from $V_G = -1$ to 0 V. The drain bias in all cases was 2 V, well into the saturation region.

Once the Taylor-series coefficients are known at each bias, the intermodulation level and the relative effect of baseband impedance on intermodulation can be predicted using (5) and (6). Graphs of the two figures-of-merits, IM3 and ΔIM3, are shown in Fig. 1.

Fig. 1(a) shows that the intermodulation varies significantly with bias. There is a sharp intermodulation null around a gate bias of –0.61 V. Fig. 1(b) indicates that in the region near this null, the intermodulation will depend strongly on the baseband impedance.

The reasons for this null and the corresponding strong baseband impedance susceptability can be seen by examining Fig. 2. The null is close to the bias where the second-order transconductance, G_{m2}, has a local maximum ($V_G \approx -0.6$). This point is also where the third-order transconductance, G_{m3}, crosses zero, be-

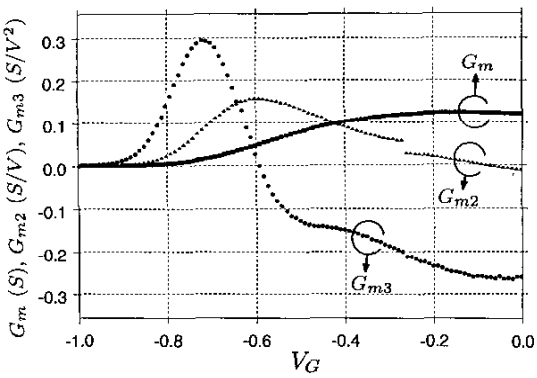

Fig. 2. The transconductance coefficients (1) of the pHEMT, at $V_D = 2$ V.

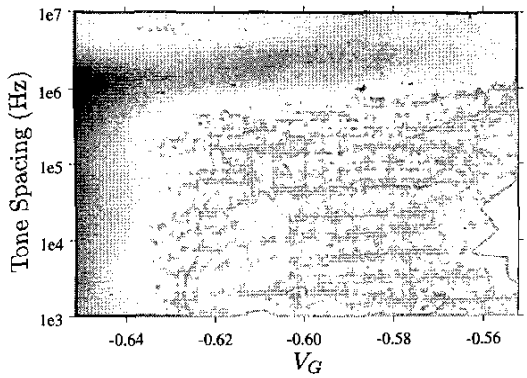

Fig. 3. Measured level of the upper intermodulation product at a fundamental frequency of 2.4 GHz. The lightest regions are at -37 dBc and the darkest regions are at -32dBc. The bias network was resonant at about 2 MHz.

cause it is the derivative of G_{m2} with respect to V_G. Thus, the third-order distortion is low, but the second-order distortion is high. As the coefficient of the intermodulation that causes baseband impedance susceptability, c_0, depends on second-order nonlinearity, the baseband impedance effects will be large at $V_G \approx -0.6$. However, the distortion for narrow bandwidth signals will be low, because $G_{m3} \approx 0$ and so $c_1 \approx 0$.

It should be mentioned that the transconductance terms alone, G_m, G_{m2} and G_{m3}, do not predict any baseband impedance effects. From [4], c_0 will be zero if the second-order cross term G_{md} and the second order conductance G_{d2} are zero. Hence, the full drain current model (1) is necessary to predict the effects of baseband impedance on intermodulation.

When ΔIM3 (Fig. 1(b)) is positive, the intermodulation level will increase as the baseband impedance increases from 0 to 50 Ω. Conversely, a negative ΔIM3 predicts a decrease in intermodulation if the baseband impedance increases. In these regions where ΔIM3 is large and negative, it is possible to cancel the intermodulation by setting the baseband impedance to a certain value, determined by (4). Hence, the common rule that the baseband impedance must be zero to achieve minimum intermodulation is not always true. This has also been observed in [6]. Also of note from Fig. 1(b) is that ΔIM3 = 0 at around $V_G = -0.3$ V, so baseband impedance will have little effect at that bias.

Distortion measurements were taken at 2.4 GHz over a range of gate biases, see Fig. 3. As predicted by Fig. 1, there is a null at $V_G = -0.61$, and the change in intermodulation due to the baseband impedance is also very large at that bias. Below this bias, the intermodulation decreases as the baseband impedance changes from 0 to 50 Ω, and the intermodulation increases for this change in baseband impedance at higher biases. Measurements at $V_G = -0.3$ confirmed that there is little change in intermodulation levels with tone spacing, because ΔIM3$\approx$0. At these high frequencies, the null is not as large as at low frequencies, and the intermodulation levels decrease with increasing gate voltage, probably because of parasitic inductive and capacitative feedback in the device.

However, the figures-of-merit (5) and (6), which are based on relatively simple low-frequency measurements, predict the trends in intermodulation levels and baseband impedance effects at high frequencies. That is, the bias regions of intermodulation nulls and high or low sensitivity to baseband impedance are accurately predicted. This method was also applied to a MOSFET and MESFET with similar results. Hence, this method can be used by a designer to select a device and its bias on the basis of intermodulation performance and susceptibility to baseband impedance effects.

IV. Predistortion Linearization Example

The effect of the baseband impedance on linearization was examined with the pHEMT operating at V_G =-0.3 and -0.6 V. As can be seen in Fig. 1(b), the dependence of intermodulation on baseband impedance is fairly large for the pHEMT device when $V_G = -0.6$ V. The intermodulation levels will have a large variation with tone spacing at that bias, because of the change in bias network impedance. At $V_G = -0.3$ V, there is little dependence on baseband impedance, so the intermodulation levels are relatively constant over a wide range of tone spacings.

The method of linearization used in this example was memoryless AM/AM AM/PM data predistortion.

The AM/AM and AM/PM characteristics were measured at $V_G = -0.3$ and -0.6 V. A complex fifth-order polynomial was fitted to the data at both biases, and the fifth-order predistorter coefficients were computed. A quadrature arbitrary waveform generator was used to generate a predistorted sinusoid, which was then modulated onto a 2.4 GHz carrier to produce a predistorted two-tone signal. The tone spacing was varied by changing the clock rate of the waveform generator.

The results of the linearization are shown in Fig. 4. At $V_G = -0.6$ V, the linearization is only useful over tone spacings less than 1 MHz because of the bias network impedance. At this bias the linearization improves the intermodulation levels by less than 9dB even at small tone spacings because the device exhibits gain expansion behavior at this bias [7], resulting in a less accurate polynomial fit.

At $V_G = -0.3$ V where baseband impedance has little impact on intermodulation, the intermodulation levels are improved by more than 13 dB over the whole range of tone spacings, Fig. 4(b). Thus, large bandwidth can be achieved using simple memoryless predistortion techniques simply by suitable selection of bias, where ΔIM3 = 0. In cases where predistortion linearization is used, selecing a bias where IM3 is high, but ΔIM3 is zero can lead to the best linearized intermodulation performance over the widest bandwidth.

V. Conclusion

A method has been proposed to enable the designer to predict the dependence of a FET's intermodulation distortion on baseband impedance over bias. Characterization of the nonlinear drain current, which can be performed relatively easily at low frequencies, is used successfully to predict the intermodulation behavior at high frequencies. This technique can be employed to compare the performance of different devices and to select a bias for the chosen device. The null in intermodulation distortion at a certain gate bias, near where many amplifiers operate, was shown to be the bias where the baseband impedance has a very large effect. In this region, memoryless predistortion linearization is effective only over narrow bandwidths where the bias network impedance does not change. However, simply by selecting the bias using the theory presented here, simple linearization is effective over wide bandwidths.

Acknowledgements

The authors thank CSIRO Telecommunications and Industrial Physics, Sydney, Australia, and Dr J. W. Archer of CSIRO for their support. James Brinkhoff is supported by an Australian Postgraduate Award.

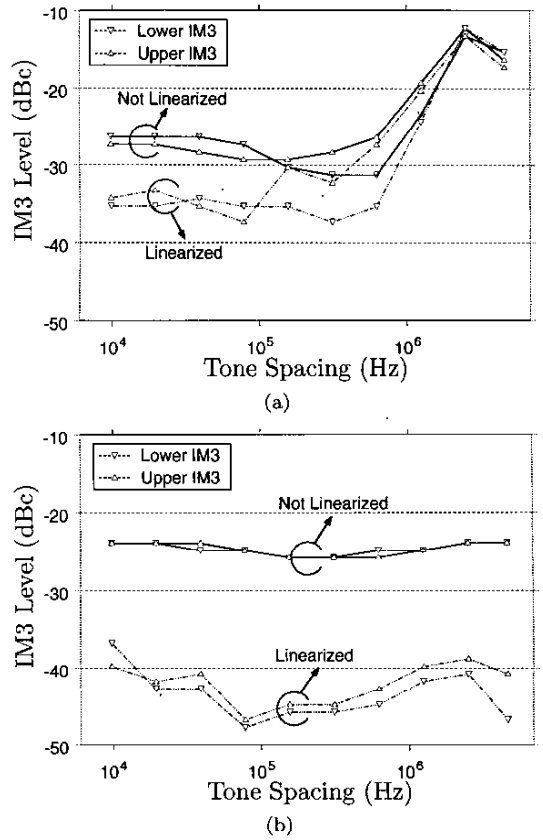

Fig. 4. Intermodulation levels for a 2.4 GHz pHEMT amplifier with and without predistortion linearization.
(a) $V_G = -0.6$ V, Fundamental output power = 5.7 dBm.
(b) $V_G = -0.3$ V, Fundamental output power = 5.2 dBm.

References

[1] W. Bosch and G. Gatti, "Measurement and simulation of memory effects in predistortion linearizers," *IEEE Trans. Microwave Theory Tech.*, vol. 37, pp. 1885–1890, Dec 1989.

[2] G. Karam and H. Sari, "A data predistortion technique with memory for QAM radio systems," *IEEE Trans. Commun.*, vol. 39, pp. 336–344, Febuary 1991.

[3] J. Vuolevi, J. Manninen, and T. Rahkonen, "Cancelling the memory effects in RF power amplifiers," in *IEEE Int. Symp. Circuits and Systems*, pp. 57–60, 2001.

[4] J. Brinkhoff and A. E. Parker, "Effect of baseband impedance on FET intermodulation," *IEEE Trans. Microwave Theory Tech.*, vol. 51, March 2003.

[5] J. C. Pedro and J. Perez, "Accurate simulation of GaAs MESFET's intermodulation distortion using a new drain-source current model," *IEEE Trans. Microwave Theory Tech.*, vol. 42, pp. 25–33, January 1994.

[6] J. F. Sevic, K. L. Burger, and M. B. Steer, "A novel envelope-termination load-pull method for ACPR optimization of RF/microwave power amplifiers," in *IEEE MTT-S Int. Microwave Symp. Dig.*, pp. 723–726, 1998.

[7] N. B. de Carvalho and J. C. Pedro, "Large- and small-signal IMD behavior of microwave amplifiers," *IEEE Trans. Microwave Theory Tech.*, vol. 47, pp. 2364–2374, Dec 1999.